Functional Roles for *N*-glycosylation of Human Carboxylesterase 1 in Hepatocellular Carcinoma Cell Line

Yun Jin Kim

The Graduate School
Yonsei University
Department of Integrated OMICS for Biomedical Science

Functional Roles for *N*-glycosylation of Human Carboxylesterase 1 in Hepatocellular Carcinoma Cell Line

A Dissertation Submitted to the Department of
Integrated OMICS for Biomedical Science and
the Graduate School of Yonsei University
in partial fulfillment of the requirements for the degree of
Master of Science

Yun Jin Kim

December 2016

This certifies that the master's thesis of
Yun Jin Kim is approved.

_____

Thesis Supervisor : Dr. Young-Ki Paik

_____

Dr. Jaewhan Song

_____

Dr. Hyun-Soo Cho

The Graduate School
Yonsei University
December 2016

CONTENTS

List of Tables

List of Figures

Abbreviations

2-D DIGE	Two-dimensional fluorescent gel electrophoresis
AFP	α-fetoprotein
CV	Crystal violet
DCP	Des-γ-carboxyprothrombin
ELISA	Enzyme-linked immunosorbent assay
GalNAc	*N*-acetylgalactosamine
GlcNAc	*N*-acetylglucosamine
HCC	Hepatocellular carcinoma
hCE1	Human liver carboxylesterase 1
IP	Immunoprecipitation
PIVKA Ⅱ	Prothrombin induced by vitamin K absence Ⅱ
RT-PCR	Real-time reverse transcription polymerase chain reaction
TM	Tunicamycin

Abstract

Functional Roles of *N*-glycosylation of Human Carboxylesterase 1 in Hepatocellular Carcinoma Cell Line

Yun Jin Kim

Department of Integrated OMICS for Biomedical Science

The Graduate School

Yonsei University

Human liver carboxylesterase 1 (hCE1) plays a central role in the xenobiotic drug metabolism and related to lipid metabolism such as triglyceride hydrolysis for normal homeostasis in liver. Glycosylation, including *N*- and *O*-linked glycan, is the most complicated post-translational modification in the biosynthesis process of proteins. The particular type of *N*-glycosylation is closely associated with the biological functions, such as cell growth, differentiation, tumor growth and cancer metastasis.

Although *N*-glycan (N79) of hCE1 is known to be related with their enzyme activity *in vitro*, its cellular function in liver cancer remains elusive. Given that hCE1 has been identified as a novel biomarker for hepatocellular carcinoma (HCC). I wanted to investigate cellular function for *N*-glycan of hCE1 in HCC. To this end, I generated hCE1 N79Q-glycan mutant stable cell line by transfecting pCMV-CES1 vector into low hCE1-expressed Hep3B origin cell line. These cells were subjected to in 2-D DIGE and LC-MS/MS for comparative proteomic analysis. From the 2-D DIGE maps, I found 71 differentially expressed protein spots (Student's *t*-Test; $p<0.05$) among which tumor

suppressor or tumor promoter was included. Interestingly, the cell growth rate in hCE1-overexpressed cells were quite lower than that of Hep3B control cells, whereas that of N79Q-glycan mutant cells were much faster than hCE1-overexpressed cells, similar to that of control cells. The lipid accumulation and hCE1 secretion assays showed that de-glycosylation of hCE1 may be not related to these phenotype changes.

Taken together, these results indicate that *N*-glycosylation of hCE1 may play an important role in anti-oncogenic role of hCE1 in liver cancer cell line.

Keyword: Hepatocellular carcinoma, human liver carboxylesterase 1, *N*-glycosylation

1. Introduction

Liver cancer is the fifth most frequently prevalent cancer worldwide and cause second cancer death (Jemal *et al*., 2011) per year. It is much more common in men than in women (Torre *et al*., 2012). Among the liver cancer types, hepatocellular carcinoma (HCC) represents the major histological subtype in primary liver cancers, accounting for 70% to 85% of the total liver cancer worldwide (Perz *et al*., 2006). One of the major problem in HCC is that there is no accurate diagnostic tool and poor prognosis with lack of symptoms in the early stages (Altekruse *et al*., 2009). More than 60% of patients are diagnosed with late-stage of HCC after metastasis has occurred, resulting in an overall 5-year survival rate of < 16% (Siegel *et al*., 2013). Findings of a previous study suggest that the early diagnosis of HCC and effective treatment are likely to prolong the lifetime of liver cancer patients (Trinchet *et al*., 2009). In the diagnosis of HCC, α-fetoprotein (AFP) is so far the most widely used tumor biomarker currently available for the early detection of HCC (Zhao *et al*., 2013). In addition, AFP-L3 which is a member of AFP glycoforms and Des-γ-carboxyprothrombin (DCP), a prothrombin induced by vitamin K absence Ⅱ (PIVKA Ⅱ), were also used for diagnosis in HCC (Tsuchiya *et al*., 2015).

Interestingly, the most-common clinically utilized serological biomarkers for cancer diagnosis and monitoring of malignant progression, as well as prognostic biomarkers of disease recurrence, are glycoproteins or carbohydrate complex (Reis *et al*., 2010). For example, HCC biomarkers (AFP, AFP-L3 and DCP), prostate cancer (PSA) (Gilgunn *et al*., 2013), breast cancer (aberrantly glycosylated MUC1) (Ebeling *et al*., 2002), and pancreatic cancer (CA19-9) (Safi *et al*., 1997).

Glycoproteins contain one or more glycans that are covalently attached to a polypeptide backbone, usually via nitrogen or oxygen linkages, in which case they are known as *N*-glycans or *O*-glycans, respectively (Varki *et al*., 2009). Glycosylation is one of the most prominent protein posttranslational modifications (PTMs) that can regulate protein functions (Zhang *et al*., 2015). The structures of *N*- and *O*-linked oligosaccharides are very different types (Lodish *et al*., 2000). The *O*-linked oligosaccharides in glycoproteins are linked to the hydroxyl group in serine (Ser) or threonine (Thr) residues by *N*-acetylgalactosamine (GalNAc). The *N*-linked oligosaccharides found in mammalian serum glycoproteins are branched and linked to the amide nitrogen of asparagine (Asn) by *N*-acetylglucosamine (GlcNAc) (Kornfeld & Kornfeld 1985).

In 2009, human carboxylesterase 1, one of *N*-linked glycoproteins, hCE1 or CES was discovered as HCC biomarker candidate in our laboratory. According to the literatures, the hCE1 was selected from those differentially expressed proteins in clinical specimens (tumor and adjacent non-tumor liver tissues) by comparative two-dimensional fluorescent gel electrophoresis (2-D DIGE) (Na *et al*., 2009). Using the real-time reverse transcription polymerase chain reaction (RT-PCR) and Western blot analysis, the mRNA and protein level of hCE1 were significantly decreased in tumor tissue than that of non-tumor tissue. Their immunohistochemistry results were well matched to those of 2-D DIGE, Western blot and RT-PCR. Taken together, hCE1 usually presents in high concentration in non-tumor tissue (normal state) but it disappears mostly in tumor tissue (Na *et al*., 2009). This result suggests that the level of hCE1 expression is highly co-related with HCC state. Even more, plasma hCE1 level detected from large number of HCC patients was much higher in HCC patients than that of control groups (e.g. healthy

donor, chronic hepatitis, liver cirrhosis, cholangiocarcinoma, gastric cancer, and pancreatic cancer) using enzyme-linked immunosorbent assay (ELISA) (Na *et al*., 2013). When the diagnostic efficiency of hCE1 was compared to that of AFP, hCE1 was shown to be much higher and thus can be used as a HCC biomarker for early detection and discrimination of HCC from other liver diseases. It was also shown that combination with AFP revealed a synergistic effect in the sensitivity and specificity (Na *et al*., 2013).

The hCE1 (CES) is known as a member of the serine hydrolase family of enzyme (E.C.3.1.1.1.) and it is also a part of the α/β fold hydrolase family (Imai 2006). This enzyme is responsible for the hydrolysis of ester- and amide-containing xenobiotics and drugs such as cocaine and heroin in liver and intestine (Satoh *et al*., 2006). In addition, other evidence suggests that some CES family enzymes may contribute to aspects of lipid metabolism through triglyceride, cholesteryl ester in fatty liver disease, not cancer state (Schreiber *et al*., 2009). Besides, hCE1 contains only one *N*-linked, high-mannose type glycosylation at residue Asn 79. This glycan site is conserved at the equivalent position in orthologues from other species. *N*-linked glycosylation seems essential for maximal catalytic activity in hCE1 for simple aromatic and aliphatic esters (Kroetz *et al*., 1993). Although hCE1 is well known as its major metabolic role in the detoxification, it has not been reported for a direct biological relationship to liver cancer and unknown whether the *N*-glycosylation of the hCE1 can influence in cellular function of hCE1 itself.

In this study, I constructed the *N*-glycan mutant stable cell line called in order to investigate the cellular functional effect of *N*-glycosylation in hCE1 itself. Either the differentially expressed proteins between hCE1-overexpressed cells and *N*-glycan mutant cells were analyzed by comparative proteomic analysis, or their protein-protein networking was performed for biological relationship using bioinformatic approaches. In

addition, I confirmed whether hCE1 is secreted by *N*-glycosylation using culture media of tunicamycin(TM)-treated and *N*-glycan mutant cells.

2. Materials and Methods

2.1. Cell lines and Cell culture

Hep3B cell line (a human hepatocellular carcinoma cell line) was obtained from ATCC (Cat#. HB-8064) and cultured in DMEM, supplemented with 10% fetal bovine serum, 100 U/mL penicillin and 100 μg/mL streptomycin. The cells were incubated at 37℃ under a humidified atmosphere of 5% CO_2 in air as a manufactural protocol (ATCC, Manassas, VA, USA).

2.2. Site-Directed Point Mutation

The pCMV-entry vector (mock control) and pCMV-CES1 vector were purchased from Origene (Rockville, MD, USA). To prepare a site directed point mutated plasmid vector of aspartic acid (N, aat) to glutamine (Q, caa), the primers were designed with point mutated oligonucleotides. PCR was performed to DNA fragment of pCMV6::CES1 using Phusion DNA polymerase (NEB, MA, USA). The primers used were: 5'-catggagctttgtgaagCAAgccacctcgtaccctc-3' (sense) and 5'- gagggtacgaggtggcTTGcttcacaa agctccatg-3' (anti-sense). After PCR is performed, it cleaved non mutated sequence by DpnI (NEB, MA, USA). The mutated expression vectors were then transformed into the *E. coli* (DH5α) for amplification and plasmid DNAs were isolated by Plasmid Maxi kit (Qiagen, Hilden, Germany).

2.3. Construction of hCE1-N79Q Glycan Mutant Stable Cell Line

5×10^6 cells per well were cultured in 100 mm dish to 80 % confluence and transfected with pCMV-CES1-N79Q cDNA using Lipofectamine 2000 (Thermo Fisher Scientific, San Jose, CA) according to the manufacturer's instructions. After transfection of cells with 5 μg of plasmid vectors, cells were continuously cultured in the presence of G418 (1 mg/mL) (Sigma,-Aldrich, Missouri, USA). G418-resistant colonies were picked, subcultured in two plates per one clone, and those cultured cells were harvested when they were reached to 80% cell confluence for hCE1 detection (Tomassi *et al*., 2003).

Cell pellets were extracted by RIPA buffer (50 mM Tris-HCl, 150 mM NaCl, 1% (v/v) Nonidet P-40, 0.5% (v/v) sodium deoxycholate, and 2 mM sodium ortho vanadate, pH 7.5) containing protease inhibitor and detection of glycans present in hCE1 was carried out by western blot analysis. Final clones were validated at least three times to ensure that hCE1 glycan mutation signal was stably expressed.

2.4. Cell Confluence Assay

The previously constructed Hep3B mock cells, hCE1-overexpressed stable cells (hCE1-OE) and hCE1-N79Q mutant cells were evaluated for their cell viability by crystal violet (CV) staining assay (protocol from Iruela-Arispe Lab, University of California-Los Angeles). The cells were fixed with 4 % paraformaldehyde (PFA) for 5 min and stained for 30 min with 0.05 % CV. After washing cells two times with distilled water, the plates were dried at 37℃ in water bath and the stained image was captured by scanner (Epson 2480, Japan).

2.5. Cell Counting Assay

Hep3B parent cells and their transformed clones (2×10^4 cells/well in 24 well plate) were cultured for 168 h with fresh media and counted in every 24 h by trypsin-EDTA treatment using a hemocytometer. The cell doubling time was estimated by a protocol available at the website (www.doubling-time.com).

2.6. Apoptosis Assay

The cell apoptosis assay was performed with Human Apoptosis Array Kit (R&D Systems, USA & Canada). Two mililiter of Array Buffer 1 serving as a block buffer was pipetted into each well of the 4-Well Multi-dish. Each array was placed into each well of the 4-Well Multi-dish and shaken for 1 h at shaking incubator. After blocking, it was replaced with 1.25 mL of Array buffer 1. The prepared sample (250 μL/array) which is composed of 400 μg of each cell lysate sample and Lysis Buffer 17 was added into prepared sample and incubated overnight at 4℃. On the next day, each array was washed with 1X Wash Buffer for 10 m.n and repeated twice times for total three washes. For each array, 15 μL of reconstituted Detection Antibody Cocktail was diluted in 1.5 mL with 1X Array Buffer 2/3. The washed arrays were shaken in the diluted Detection Antibody Cocktail for 1 h. Each array was washed with Wash Buffer as above and incubated for 30 min with a 1:2000 dilution of the secondary antibody to 1X Array Buffer 2/3. The signal was detected using ECL Plus Western blotting detection reagents (GE Healthcare, Uppsala, Sweden) (protocol from R&D systems, cat.ARY009).

2.7. 2-D DIGE and Image Analysis

For 2-D DIGE, the cell pellets were extracted using 2D lysis buffer (7 M urea, 2 M thiourea, 4% CHAPS, 30 mM Tris, pH 8.5) with protease inhibitor as described previously (Na *et al*., 2009). Fifty microgram of each sample and a pooled internal standard were cross-labeled with 400 pmol of Cy3, Cy5 and Cy2 fluorescent dye, respectively (GE Healthcare, Uppsala, Sweden). This internal standard was labeled with Cy2 and was run in parallel with Hep3B mock, hCE1-OE and hCE1-N79Q cell lysate samples. The labeling reaction was carried out in the dark and iced condition for 30 min and quenched with 10 mM lysine for 10 min. After quenching, labeled samples were combined, rehydrated, isoelectrically focused with 24 cm Immobiline Dry Strip pH 3-10NL (GE Healthcare, Uppsala, Sweden). The IPG strips were reduced and alkylated in a single step by incubation in Equilibration buffer (6 M Urea, 2% SDS, 30 mM Tris, 20% glycerol, 2.5% acrylamide solution) with 5 mM Tributylphosphine (TBP), and finally separated in the second dimensional by SDS-PAGE (9~16%) on an Ettan DALT 12 system (GE Healthcare, Uppsala, Sweden). The CyDye-labeled gels were scanned on a Typhoon 9400 scanner (GE Healthcare, Uppsala, Sweden) at the manufacturer's recommended excitation/emission wavelengths. The gel images were analyzed using DeCyder 2-D analysis software v6.5.11 (GE Healthcare, Uppsala, Sweden). Gel spot matching and statistical analysis were carried out using the Biological Variance Analysis (BVA) module. A spot was accepted as statistically significant if $p < 0.05$ and had a cut off-ratio greater than ±1.3-fold as differentially expressed spots in mock versus hCE1-OE or mock versus hCE1-N79Q sample (The protocol adopted at Aberdeen Proteomics for 2-D DIGE).

2.8. 2-D Gel Electrophoresis for the Preparative Gel

Total 1.2 mg of the non-labeled internal standard was rehydrated, focused, and transferred to the second dimension as described for 2-D DIGE procedure. The preparative gel was stained with Coomassie Brilliant Blue G250 (CBB) solution for overnight, destained using ultrapure distilled water, and then scanned by GS 710 scanning densitometer (Bio-Rad, Hemel Hempstead, U.K.).

2.9. Trypsin Digestion

The selected spots were picked and transferred into each 1.5 mL tube. The spots were washed with 100 μL of distilled water; then, 50 μL of 50 mM NH_4HCO_3 (pH 7.8) and acetonitrile (6:4, v/v) were added and mixed for 10 min. This process was repeated at least three times until the CBB dye disappeared. The supernatant was decanted, and the spots were dried in speed vacuum concentrator (LaBoGeneAps, Lynge, Denmark) for 10 min. The protein into spot was treated and digested with 20 ng per spot of trypsin (Promega, Southampton, U.K.) in 50 mM NH_4HCO_3. Spots were left on ice condition for 45 min and incubated at 37℃ for 12 h. Trypsin digested solution was collected into fresh 1.5 mL tube, evaporated and then stored in -70℃ (The protocol of trypsin digestion of proteins in solution are adapted from Promega).

2.10. LC-MS/MS for Protein Analysis

Nano LC-MS/MS analysis was performed with Easy n-LC (Thermo Fisher San Jose, CA, USA) and a LTQ Orbitrap XL mass spectrometer (Thermo Fisher, San Jose, CA, USA) equipped with a nano-electrospray source. Samples were separated on A C18 nanobore column (150 mm × 0.1 mm, 3 μm pore size; Agilent). The mobile phase A for LC separation was 0.1% formic acid, 3% acetonitrile in deionized water and the mobile phase B was 0.1% formic acid in acetonitrile. The chromatography gradient was designed for a linear increase from 0% B to 32% B in 23 min, 32% B to 60% B in 3 min, 95% B in 3 min, and 3% B in 6 min. The flow rate was maintained at 1500 nL/min. Mass spectra were acquired using data-dependent acquisition with a full mass scan (350–1200 m/z) followed by 10 MS/MS scans. For MS1 full scans, the orbitrap resolution was 15,000 and the AGC was 2×10^5. For MS/MS in the LTQ, the AGC was 1×10^4 (Lee *et al*., 2014).

2.11. Data Searching for Protein Identification

The mascot algorithm (Matrixscience, USA) was used to identify peptide sequences present in a protein sequence database. Database search criteria were, taxonomy; Homo sapiens (downloaded; 20160728) fixed modification; carbamidomethylated at cysteine residues; variable modification; oxidized at methionine residues, maximum allowed missed cleavage; 2, MS tolerance; 10 ppm, MS/MS tolerance; 0.8 Da. The peptides were filtered with a significance threshold of $p<0.05$ (Lee *et al*., 2014).

2.12. Protein Networking by Database classification

Protein network and Gene Ontology (GO) of the differentially expressed proteins were performed using STRING database version 10.0 (string-db.org) and PANTHER as bioinformatics resources. The groups with similar functional annotations were classified into graphic color (www.pantherdb.org).

2.13. Western Blot Analysis

Sample was separated by SDS-PAGE (10%) and transferred onto nitrocellulose membranes using an iBLOT dry blotting system (Invitrogen, Carlsbad, CA, USA). The membranes were blocked for 1 h with TBS-T buffer (20 mM Tris, 137 mM NaCI, 0.1% Tween-20, 5% Skim milk, pH 7.6), incubated for overnight with a 1:2000 dilution of a polyclonal anti-hCE1 antibody (Abcam, Cambridge, UK), and then incubated for 1 h with a 1:2000 dilution of horseradish peroxidase-conjugated goat anti-rabbit secondary antibody (Santa Cruz, La Jolla, CA, USA). For immunoprecipitation (IP), sample protein was mixed with protein G agarose bead (Thermo Fisher Scientific, San Jose, CA) and target primary antibody (1:10, v/v). After reacting for overnight at 4℃, the beads were washed with PBS-T, and antibody-binding protein was eluted using 100 μL PBS adjusted to pH 2. The eluent was neutralized and then concentrated *in vacuo*. The dried pellet was dissolved in 20 μL of 2D lysis buffer and the solution was applied to Western blot analysis as described above. Immunoreactive proteins were detected using ECL Plus Western blotting detection reagents (GE Healthcare, Uppsala, Sweden) and Typhoon scanner (GE Healthcare, Uppsala, Sweden). The signal intensity was estimated

densitometrically using ImageQuant TL v2005 software (GE Healthcare, Uppsala, Sweden) (Na *et al*., 2009).

2.14. Oil Red O Staining Analysis

5×10^5 cells were cultured in 6-well plates to 80 % confluence and fixed for 30 min with 4 % PFA at 4℃. After washing three times with PBS, added 4 % PFA for 10 min and incubated cells with renewed 4% PFA in dark condition at room temperature (RT). PFA was removed and added 60% isopropanol for 5 min. They were removed and dried on 37℃ water bath. Oil Red O working solution was added and incubated for 10 min at RT. After washing four times with distilled water, the stained image was visualized through a microscope (XI-71-F22PH, Olympus) (The protocol was prepared by Roy Ellis, Woodville, South Australia).

2.15. De-glycosylation by Tunicamycin Treatment

The hCE1-OE clone (5×10^5 cells) was incubated in 100 mm dish with OPTi-MEM (Thermo Fisher Scientific, San Jose, CA). After 12 h incubation, Tunicamycin (TM) was treated to 0.1 ~ 1.0 μg/mL and additionally incubated for 24 h. The cell pellets and its media were collected by centrifuge at 5,000 rpm. The cells were extracted by RIPA buffer and media was concentrated by 3 kDa filter. The de-glycosylation of hCE1 was validated by western blot analysis (Nonaka *et al*., 2007).

3. Results

3.1. Construction of hCE1-N79Q Glycan Mutant Stable Cells

Before hCE1 *N*-glycan mutant stable cell line was established, the de-glycosylation of hCE1 was confirmed by direct transfection using pCMV-empty, pCMV:hCE1 and pCMV:hCE1-N79Q vector (Fig. 1). The previously constructed mock control and hCE1-OE clones showed that hCE1 was expressed in hCE1-OE cells, but not in mock control (Fig. 2A). In the direct transfection of plasmid vectors, hCE1 was overexpressed in transient cells with pCMV:hCE1 and pCMV:hCE1-N79Q vector, and hCE1 signal expressed by pCMV:hCE1-N79Q vector was slightly decreased (Fig. 2B). The results suggest that the vectors are suitable for de-glycosylation of hCE1.

The clones of the hCE1-N79Q glycan mutant stable cells were selected from colony selection by G418 treatment and continuously cultured for 3 months. Total five candidates were selected as N79Q mutant cell clones (N79Q-1 ~ N79Q-5), and their hCE1 levels were detected by western blot analysis. The results showed that N79Q-1 and N79Q-5 clones verify stable transfection condition, which are hCE1 overexpression and sift down of hCE1 position (Fig. 2C). In hCE1-OE cell line, molecular weight (MW) of the hCE1 signal was higher than natural hCE1 form (nhCE1, untagged) which is purified from liver tissue since the C-terminal of hCE1 in pCMV:hCE1A1 vector was DDK-tagged (25 amino acid). In the case of the hCE1-N79Q cell line, the glycan site in same pCMV:hCE1A1 vector was mutated and then the hCE1 signal was shown shift-downed molecular weight than that of hCE1-OE cells (upper signal band).

3.2. Measurement of Cell Proliferation and Doubling Time

When comparison was made for the cell morphologies between Hep3B parental cells and their stable cells, hCE1-N79Q-1 cells were shown to be round shape than that of either mock control or hCE1-OE cells (Fig. 3A). In order to compare the basic cell characterization, cell proliferation assay was performed by counting cell numbers for 8 days. As a result, hCE1-OE cell number was decreased than that of either Hep3B parental cells or mock cells, while hCE1-N79Q-1 cell number was increased than that of hCE1-OE cells (Fig. 3B). When the cell doubling time from their final cell numbers during 8 days was estimated, the doubling time of hCE1-OE cells were increased compared to that in Hep3B parental cells and mock cells, and that of hCE1-N79Q-1 cells were decreased compared to that in hCE1-OE cells, interestingly similar to Hep3B parental cells (parental, 40.4 h; Mock, 43.6 h; hCE1-OE, 58.7 h; hCE1-N79Q-1, 37.7 h) (Fig. 3C). This result suggests that the glycan structure of hCE1 might have influence the morphological change and their cell growth.

3.3. Relationship to Cell Apoptotic Factor

To investigate differences in apoptosis-related proteins between Hep3B parental and stable cells, I performed the apoptosis assay using Human Apoptosis Array kit. In thirty-five apoptosis-related proteins, four proteins (Bax, TRAIL R2/DR5, phospho-p53 (Ser15) and phospho-p53 (Ser392)) had difference more than ±50 % between mock cells and hCE1-OE cells, or mock cells and hCE1-N79Q-1 (Fig. 4). This indicates that the difference of cell growth rate between hCE1-OE and hCE1-N79Q-1 might be influenced

by changes in those apoptotic factors.

3.4. Proteomics Analysis of the Differentially Expressed Proteins between the Mutant Hep3B Stable Cells

To identify those cancer-related proteins that have been changed in their expression between Hep3B stable cells, 2-D DIGE analysis was performed. The differentially expressed spots were statistically analyzed from four florescent gels (Fig. 5A), which resulted in total 71 spots having significantly different expression (p<0.05, over ±1.3-fold) that were identified and quantified by LC-MS/MS (Fig. 5B). The identified proteins were divided into six groups of increased and/or decreased patterns (Fig. 6). The hCE1-N79Q-1 cells were slightly differed for mock cells and hCE1-OE cells (Fig. 6A and 6B). In Figure 6C and 6D, the pattern of mock cells versus hCE1-OE cells was significantly decreased, whereas that of hCE1-N79Q-1 cells versus hCE1-OE cells remained unchanged. However, that of hCE1-N79Q-1 cells versus hCE1-OE cells were significantly decreased or increased (Fig. 6E, F). These results indicate that *N*-glycosylation of hCE1 might have influenced protein expression of pattern E and F. The identified proteins corresponding to their patterns is listed in Table 1–6.

3.5. Protein Networking and Related Biological Functions by De-glycosylation of hCE1

To investigate the correlation between differentially expressed proteins and their biological function as well as protein-protein networking, the PANTHER and STRING as

bioinformatic databases were used. Their biological function was presented as catalytic activity (32.6%), cell structural molecule (24.3%), nucleic acid binding transcription factor (15.9%), receptor activity (9.0%), protein translation regulator (8.7%), calmodulin signal pathway (7.8%) and enzyme regulator (2.2%) (Fig. 7A). The protein-protein networking groups were divided into energy metabolism, cell structure molecule and proliferation, ATP synthesis, nucleic acid binding transcription factor, and protein translation regulator (Fig. 7B).

Among those 71 identified proteins, the level of representative cancer-related protein (e.g. Annexin IV) was validated by western blot analysis. In 2-D DIGE results, Annexin IV level was increased than either that of mock or hCE1-OE cells (Table 6, Fig. 8A and 8B) and also increased in western blot validation result (Fig. 8C).

3.6. Effect of De-glycosylation of hCE1 on Lipid Hydrolysis

Since it is well known that the hCE1 has catalytic function of lipid hydrolysis in intracellular state, I performed the lipid accumulation assay of each cell line by Oil red O staining. Hep3B parental and mock cells showed the similar lipid accumulated droplets (Fig. 9A and 9B), whereas hCE1-OE cells showed remarkably reduced level of lipid droplets compared to that of parental and mock cells (Fig. 9C). However, there was no difference in lipid accumulation between hCE1-N79Q-1 and hCE1-OE cells (Fig. 9D). Based on these results, it was concluded that the *N*-glycan structure of hCE1 may not be related to cellular lipid metabolism.

3.7. Effect of *N*-glycosylation of hCE1 in Protein Secretion

Tunicamycin (TM) was known as specific inhibitor of *N*-glycosylation enzyme in intracellular state. Before N79Q stable cell line is constructed, TM treatment of hCE1-OE cells was performed and their hCE1 signal was validated by Western blot analysis. In TM-treated hCE1-OE cell lysates, the MW of hCE1 was shift-downed and the secreted hCE1 in cell media was also detected (below of double band) (Fig. 10A). The shift-downed MW position of de-glycosylated hCE1 of hCE1-N79Q-1 and N79Q-5 cells was re-confirmed by same position of TM treatment cells (Fig. 10B). In both cell lysates and media of two hCE1-N79Q cells, hCE1 was detected (Fig. 10C). Taken together, these results suggest that glycosylation at N79 (of hCE1) does not appear to influence the secretion of hCE1 protein.

4. Discussion

De-glycosylation and Cell Growth

As the changes in the *N*-glycan core on the surfaces of many cancer cells are known to be association with cellular oncogenesis (Hua *et al*., 2014), (e.g. *N*-glycan of FUT8 for biomarker in evaluating HCC cell progression) (Cheng *et al.,* 2016), the increase in the cell doubling time of hCE1-N79Q clone over that in Hep3B mock control cells suggests that *N*-glycan structure of hCE1 may have strong correlation with character of the cancer cells. From array analysis for 35 apoptotic factors, three proteins (Bax, TRAIL R2/DR5 and phosphorylated p53) were increased or decreased in hCE1-N79Q clone (Fig. 4). Bax is known as an important protein of apoptosis as a part of Bcl-2 family that regulates the cell life and death (Fulda *et al*., 2006), and it causes apoptosis in cancer cell (Reed *et al*., 2006). TRAIL R2/DR5 is known as a death receptor and is activated by ligand, which causes tumor necrosis factor-related apoptosis and transforms apoptosis signal (Rajeshkumar *et al*., 2010). DR5 targeting monoclonal antibody was treated as drug Tigatumab in pancreatic cancer (Forero-Torres *et al*., 2013). The p53 is well known as a tumor suppressor and transcription factor and the activation of p53 induce cell cycle arrest and DNA repair or apoptosis (Cuddihy *et al*., 1999). When DNA damage is generated in cellular environment, the p53-S15 phosphorylation is induced. By their results, S15 targets the ubiquitination and proteasomal degradation and inhibit interaction with MDM2 which inhibit accumulation of p53. The p53-S392 phosphorylation by cyclin-dependent kinases regulating cell cycle progression was increased in human tumor and affect growth suppressor function and transcriptional activation of p53 (Cox *et al*.,

2010). Taken together, I think that *N*-glycan of hCE1 may affect cell proliferation significantly by regulation of these apoptotic factors. However, it remains to validate the detailed mechanism underlying such anti-oncogenic activity of hCE1.

Effect of De-glycosylation of hCE1 on the Expression of Cellular Proteins

From the 2-D DIGE proteomics analysis, many differentially expressed protein spots of [mock control vs. hCE1-OE vs. hCE1-N79Q clone] were visually shown in fluorescence images, indicating when these proteins were classified, the effect of *N*-glycosylation of hCE1 on the expression of many proteins appear to influence positively on the cellular oncogenes (e.g. invasion, migration of HCC or lung cancer). These proteins belong to pattern A, some of protein such as S100A11, YWHAG and ACTN4 was as promoter of cell (Luo *et al*., 2013; Ko *et al*., 2011; Wang *et al*., 2015). In addition, EIF4E was increased in HCC tissues and its expression level has strong correlation with tumor recurrence (Wang C *et al.* 2015). Besides, it was reported that the expression of XRCC5 (Ku80) and HRNR is related to the tumor progression (Pucci *et al*., 2004, 2009; Fleming *et al*., 2012), and EF2 is overexpressed in stomach and colorectal cancer (Nakamura *et al*., 2009). Those proteins belong to pattern B, there are several proteins involved in oncogenesis or other cellular processes. For example, knockdown of the HNRNPL inhibits migration and invasion in HCC cell line (Yau *et al*., 2013), and fumarase hydratase and HNF4A are related to HBV and down-regulated in liver cancer cell (Zhang *et al*., 2009; Ning *et al*., 2010). The inhibition of ATP6V1E1 decreases cell growth and metastasis in HCC cell line (Lu *et al*., 2012), and KARS is related to the inflammation with stomach cancer. FABP1 is not related to the cancer, but known as cytosolic protein which is transport fatty acid and decreased cell damage from hypoxia/

reoxygenation (Elchuri *et al*., 2007). These proteins belong to pattern C, several proteins are found to be involved in other cellular processes. For example, S100A6 has correlation with cellular processes such as cell proliferation, differentiation, migration and cytoskeletal dynamics in HCC cell line (Hua *et al*., 2011), while Annexin A2 is major role of liver cancer progression that was significantly up-regulated in HCC tissue (Ji *et al*., 2009). For those proteins belong to pattern D, M6PR was known as receptor and affected promotion of division in HCC development (Scharf *et al*., 2001), while FABP5 was as promoter for cell proliferation, migration and invasiveness (Ohata *et al*., 2015). For those proteins belong to pattern E, STMN1 promotes tumor cell invasion (Hsieh *et al*., 2010), and PCNA was reported that it was significantly increased in liver cancer (Mun *et al*., 2006), and the expression level of GRB2 was increased in HCC tissue against non-tumor tissue and has strong correlation with progress and prognosis of HCC patients (Zhang *et al*., 2013). Besides, TPM3 and SOD2 as tumor suppressor significantly decrease tumorigenesis of cell migration and invasion in HCC cell line (Choi *et al*., 2010; Yi *et al*., 2011). For those proteins belong to pattern F, hCRNN4 (coronin) is overexpressed in HCC tissue and it enhances the cell migration (Wang *et al*., 2013). ANXA4 also promotes progress of HCC (Wei *et al*., 2015). ERP29 was known as oncogenic factor for invasion of breast cancer (Bambang *et al*., 2009). In expression pattern A–C, the proteins of [mock control vs. hCE1-OE] had significant difference, but the proteins of [hCE1-OE vs. hCE1-N79Q] had no significant difference. It means that there is no association for glycosylation on original function of hCE1. On the other hand, the proteins of expression pattern D–F have remarkable increase- and/or decrease-patterns. Taken together, these protein information indicates that *N*-glycosylation of hCE1 might be effect on the main function that hCE1 regulate cancer-related proteins expression.

N-glycosylation and Extracellular Secretion

Regarding the correlation of *N*-glycosylation and secretion, many studies has been previously published. The majority of secretory proteins undergo asparagine-linked (*N*-linked) glycosylation during their ER transit (Barbara *et al*., 1995). First, a preassembled core oligosaccharide is attached to the Asn residue of the Asn-Xaa-Ser/Thr motif (sequon) in the nascent polypeptide chain entering the ER lumen (Bause *et al*., 1983). The oligosaccharide promotes protein folding by increasing stability and preventing aggregation (Shental-Bechor *et al*., 2009). The core glycan undergoes further modifications in the ER and Golgi and the resulting glycan structure provides information for quality control and intracellular trafficking within the secretory pathway (Helenius *et al*., 2001). *N*-linked glycosylation can also influence the stability of folded (Lederkremer *et al*., 2009), mature proteins and may modify protein function including catalytic activity of enzymes and ligand binding to receptors (Skropeta *et al*., 2009). For example, *N*-linked glycosylation of human CTRC is required for efficient folding and secretion, however, the *N*-linked glycan is unimportant for enzyme activity or inhibitor binding (Bence & Sahin-Tóth 2011). Also, the *N*-glycan of EC-SOD is essential for its secretion and may be involved in the pathogenesis of the diseases, such as cardiovascular disease or COPD (Ota *et al*., 2016). However, the *N*-glycosylation of hCE1 might not be affect secretion in our results. Therefore, I hypothesize that the other transport regulator or exosome may be affect secretion of hCE1.

Table 1. List of Identified proteins corresponding to Figure 6A

Accession No.	Protein name	Ratio (N79Q/OE)	*p* value	MS Score
gi|2804273	Alpha actinin 4 (ACTN4)	1.01	0.033	239
gi|31106	Elongation factor 2	1.17	0.04	464
gi|2984586	TERA	1.09	0.031	43
gi|412172	Villin (VIL1)	1.03	0.052	939
gi|125731	X-ray repair cross-complementing protein 5 (XRCC5)	1.19	0.066	591
gi|6456472	Prolyl endopeptidase (PREP)	1.23	0.15	249
gi|31707	GDH (GLUD1)	1.06	0.051	230
gi|28346	Actin-related protein	1.00	0.034	187
gi|40795897	Hornerin precursor (Hornerin; HRNR)	-1.09	0.015	721
gi|157833780	Human Annexin V With Proline Substitution By Thioproline (ANXA5)	-1.20	0.0063	298
gi|998357	EB1 (MAPRE1)	-1.24	0.0096	272
gi|23222	14.3.3 protein (YWHAG)	1.00	0.016	243
gi|306487	Cap-binding protein (Eukaryotic Translation Initiation Factor 4E; EIF4E)	-1.04	0.014	156
gi|2282042	p16-Arc (ARPC5)	1.00	0.029	375
gi|553734	Putative	-1.24	0.00085	49
gi|34343	Unnamed protein product	-1.41	0.0095	55
gi|560791	Calgizzarin (S100 Calcium Binding Protein A11; S100A11)	-1.56	0.0011	82

Table 2. List of Identified proteins corresponding to Figure 6B

Accession No.	Protein name	Ratio (N79Q/OE)	*p* value	MS Score
gi|62113341	Serum albumin (ALB)	1.23	0.0026	554
gi|2366752	Lysyl tRNA Synthetase (KARS)	-1.17	0.0057	1095
gi|1353248	Pyrroline-5-carboxylate dehydrogenase	1.31	0.0039	230
gi|20151189	Chain A, Structure Of Human Glutamate Dehydrogenase-Apo Form	1.38	0.022	688
gi|31707	GDH (GLUD1)	1.57	0.13	157
gi|182794	Fumarase precursor (Fumarate Hydratase; FH)	-1.04	0.036	277
gi|35038	Nuclear factor IV (Hepatocyte Nuclear Factor 4, Alpha; HNF4A)	1.52	0.026	82
gi|531391	Acyl-CoA dehydrogenase (ACADSB)	1.14	0.018	170
gi|3941342	Mitochondrial outer membrane protein (TOMM40)	1.03	0.037	206
gi|1770576	Translin associated protein X (TSNAX)	-1.27	0.008	367
gi|417719	40S ribosomal protein S3 (RPS3)	1.56	0.00054	155
gi|313014	Vacuolar proton ATPase (ATP6V1E1)	1.43	0.03	211
gi|6018458	6-phosphogluconolactonase (PGLS)	1.05	0.051	71
gi|963048	Caseinolytic Mitochondrial Matrix Peptidase Proteolytic Subunit (CLPP)	1.28	0.0016	220
gi|682748	Antioxidant protein 1 (ATOX1)	-1.35	0.02	318
gi|28317	Unnamed protein product	1.46	0.025	178
gi|119808	Fatty acid-binding protein (FABP1)	-1.08	0.011	80
gi|28318	Unnamed protein product	1.34	0.022	82
gi|11527777	Heterogeneous nuclear ribonucleoprotein L (HNRNPL)	-1.15	0.0013	123

Table 3. List of Identified proteins corresponding to Figure 6C

Accession No.	Protein name	Ratio (N79Q/OE)	*p* value	MS Score
gi|125731	X-ray repair cross-complementing protein 5 (XRCC5)	1.21	0.0033	299
gi|113950	Annexin A2 (ANXA2)	1.77	0.097	657
gi|40795897	Hornerin precursor (Hornerin; HRNR)	1.26	0.001	401
gi|113954	Annexin A3 (ANXA3)	1.62	0.027	509
gi|28317	Unnamed protein product	1.38	0.049	308
gi|116509	S100 Calcium Binding Protein A6 (S100A6)	1.76	0.029	49

Table 4. List of Identified proteins corresponding to Figure 6D

Accession No.	Protein name	Ratio (N79Q/OE)	*p* value	MS Score
gi|48146385	EIF3S4 (Eukaryotic Translation Initiation Factor 3, Subunit G; EIF3G)	2.00	0.097	186
gi|3095186	Cargo selection protein TIP47 (Mannose-6-Phosphate Receptor; M6PR)	1.58	0.0012	67
gi|435476	Cytokeratin 9 (KRT9)	2.02	0.00063	367
gi|267187	Splicing factor U2AF 35 kDa subunit	2.20	0.0044	103
gi|182354	Fatty Acid Binding Protein 5 (FABP5)	2.07	0.15	82
gi|28317	Unnamed protein product	2.21	0.0022	2

Table 5. List of Identified proteins corresponding to Figure 6E

Accession No.	Protein name	Ratio (N79Q/OE)	*p* value	MS Score
gi|54648253	KH-Type Splicing Regulatory Protein (KHSRP)	-1.20	0.01	216
gi|595410	Guanosine 5'-monophosphate synthetase (GMPS)	-1.50	0.087	863
gi|129694	Proliferating cell nuclear antigen (PCNA)	-1.43	0.097	374
gi|12653955	Tropomyosin 3 (TPM3)	-2.00	0.023	383
gi|181976	Epidermal growth factor receptor-binding protein (GRB2)	-1.57	0.016	209
gi|1330301	Mn-superoxide dismutase (SOD2)	-1.41	0.004	239
gi|4929705	Mitochondrial Ribosomal Protein L48 (MRPL48)	-1.77	0.043	147
gi|35595	Pr22 protein (Stathmin 1; STMN1)	-2.24	0.011	475
gi|28317	Unnamed protein product	-1.48	0.0032	177
gi|184565	Transformation-sensitive protein (Stress-Induced Phosphoprotein 1; STIP1)	-1.55	0.066	725

Table 6. List of Identified proteins corresponding to Figure 6F

Accession No.	Protein name	Ratio (N79Q/OE)	p value	MS Score
gi|5701731	hCRNN4 (Coronin; CORO1C)	1.48	0.045	637
gi|119607256	Keratin 8 Pseudogene 3 (KRT8P3)	2.37	0.0026	507
gi|347314	Heterogeneous Nuclear Ribonucleoprotein H1 (HNRNPH1)	1.62	0.12	518
gi|530369362	POTE ankyrin domain family member F isoform X1 (POTEF)	1.48	0.00049	129
gi|178699	Annexin IV (placental anticoagulant protein II; ANXA4)	1.42	0.041	452
gi|2393722	Glutathione S-Transferase Omega 1 (GSTO1)	1.54	0.093	498
gi|12803813	DCI protein (Enoyl-CoA Delta Isomerase 1; ECI1)	1.36	0.03	352
gi|3413293	Endoplasmic Reticulum Protein 29 (ERP29)	1.27	0.026	304
gi|130850	Proteasome subunit alpha type-2 (PSMA2)	1.19	0.048	168
gi|682748	Antioxidant 1 Copper Chaperone (ATOX1)	1.37	0.012	267
gi|14327972	Mesoderm Development Candidate 2 (MESDC2)	1.19	0.14	139
gi|28317	Unnamed protein product	2.11	0.04	78

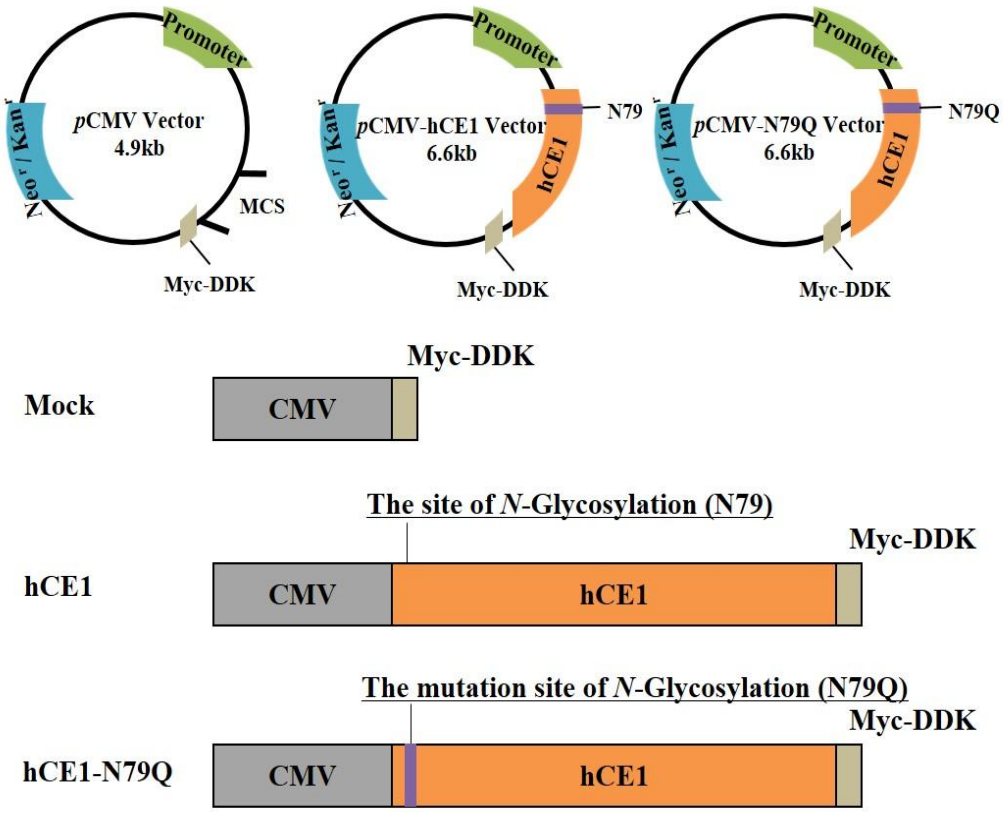

Figure 1. Structure of cDNA plasmid for the site-directed point mutation.

Cloning was performed using empty vectors which have CMV promoter and then, hCE1 was inserted into multiple cloning site by DNA ligase. To transform asparagine in 79th site into glutamine, *N*-glycan mutant vector was constructed by using Dpn I enzyme with site-directed protein mutation methods and then each vector was transfected into parental Hep3B cells. After G418-resistant colony selection, mock, hCE1-OE1, and hCE1-N79Q cells were confirmed from stably hCE1 expression by Western blot.

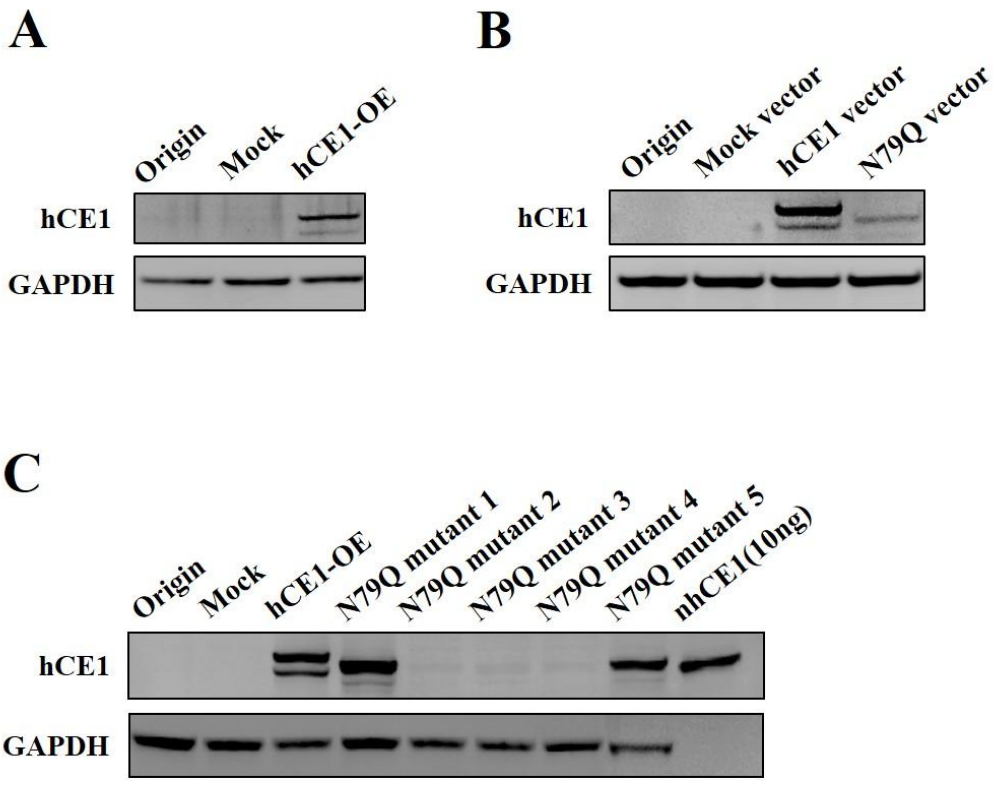

Figure 2. Stable cell induction and hCE1 expression.

(A) The hCE1 level in hCE1-OE cell was highly overexpressed over Hep3B parental and mock control cells. (B) To test the efficiency vector transfection, three vectors were directly transfected into Hep3B parental cells and their increased hCE1 level was confirmed by western blot. (C) Among the five *N*-glycan mutant stable cell clones, hCE1-N79Q-1 and hCE1-N79Q-5 clone showed hCE1 overexpression and shift-down of its molecular weight. The two *N*-glycan mutants were validated as a stably hCE1-expressed cell line by triplicate-repeated immunoblot.

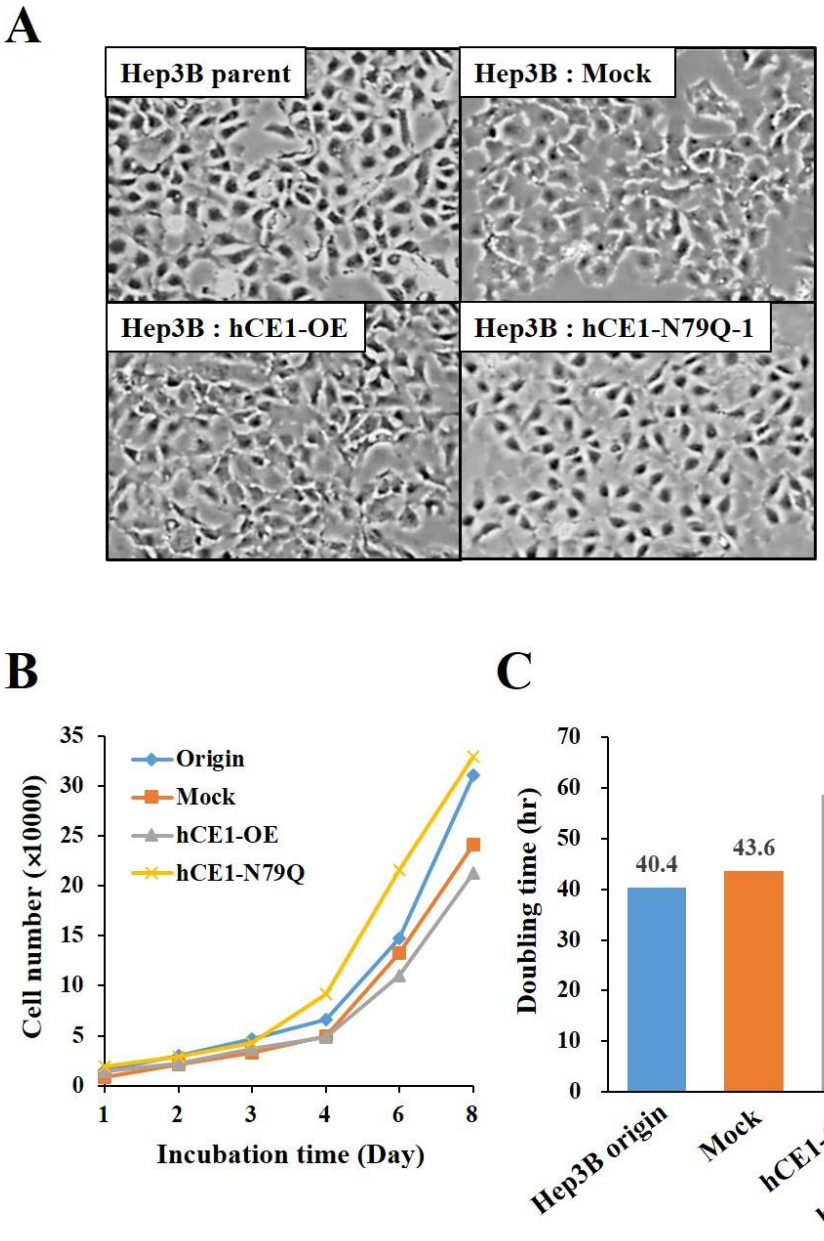

Figure 3. Stable cell morphology and cell proliferation.

(A) Differences in cell morphology among Hep3B parental, mock control, hCE1-OE and hCE1-N79Q-1 clones. The cloned cells show more constant mono-cell shape. (B) Cell proliferation was determined from cell counting by hemocytometer and (C) their cell doubling time was estimated by first seeding cell number to final cell number (0–168 h).

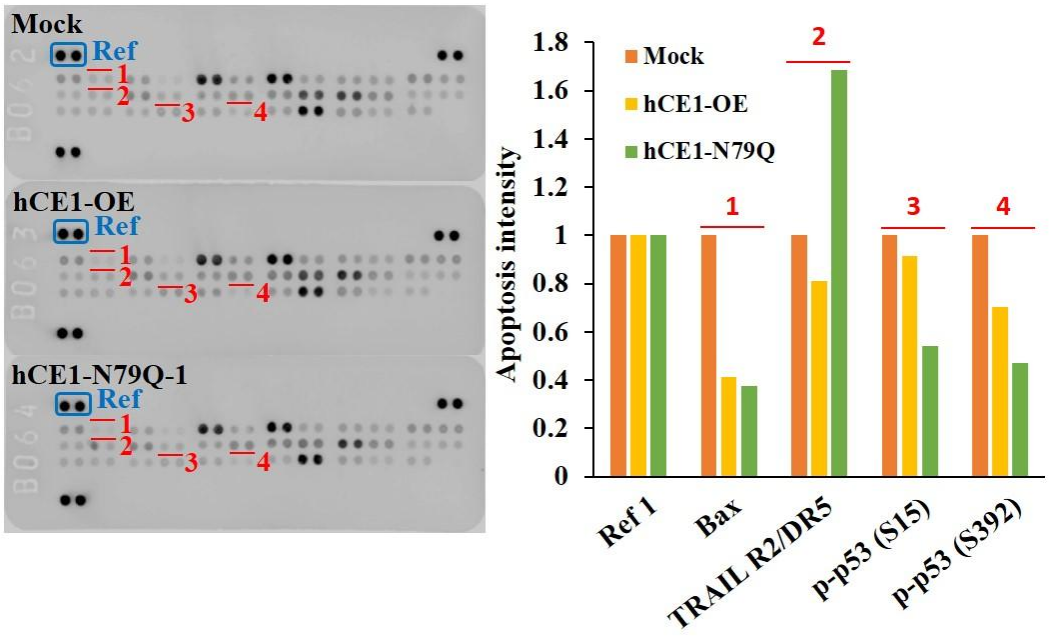

Figure 4. Effect of de-glycosylation of hCE1 on apoptotic factors.

Differentially expressed apoptotic proteins of mock, hCE1-OE and hCE1-N79Q-1 clones were analyzed by using 35 antibody apoptosis array kit. The intact two spots are the same protein and the ratio was estimated by calculating the reference average intensity (square, left panel). Four differentially expressed proteins were presented against indicating number (right panel).

A

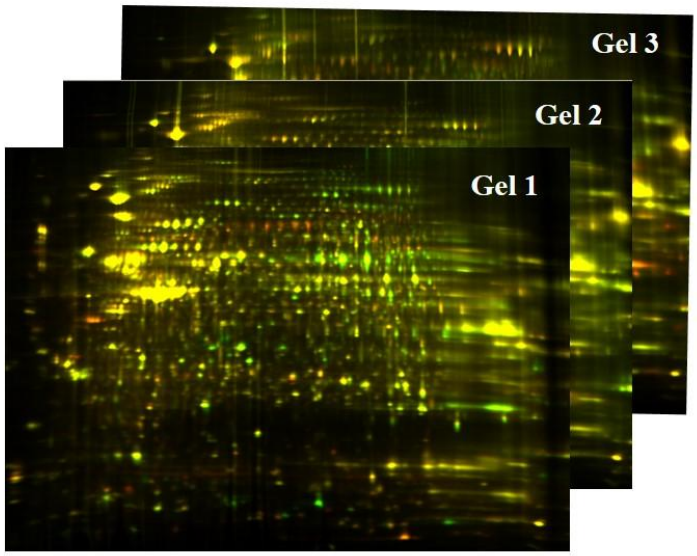

B

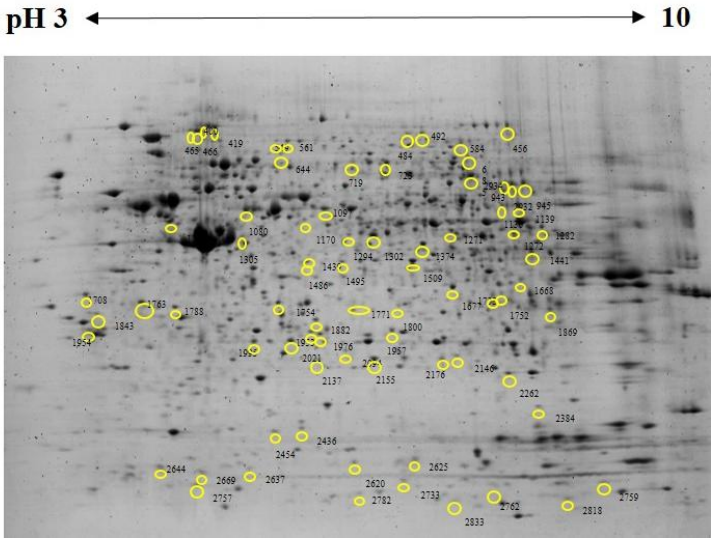

Figure 5. Comparative proteomic analysis of cell transfected with expression vector harboring de-glycosylation of hCE1.

Mock control, hCE1-OE and hCE1-N79Q-1 cell lysates were labeled with Cy3 or Cy5, and followed through 2-DE process (duplicates). (A) The labeled gels were scanned and Cy3/Cy5-labeled images were merged. (B) The seventy one differentially expressed spots (Student's *t*-Test; $p<0.05$) were highlighted in the preparative 2-D gel image. They were excised and subjected to in-gel trypsin digestion for LC-MS/MS analysis.

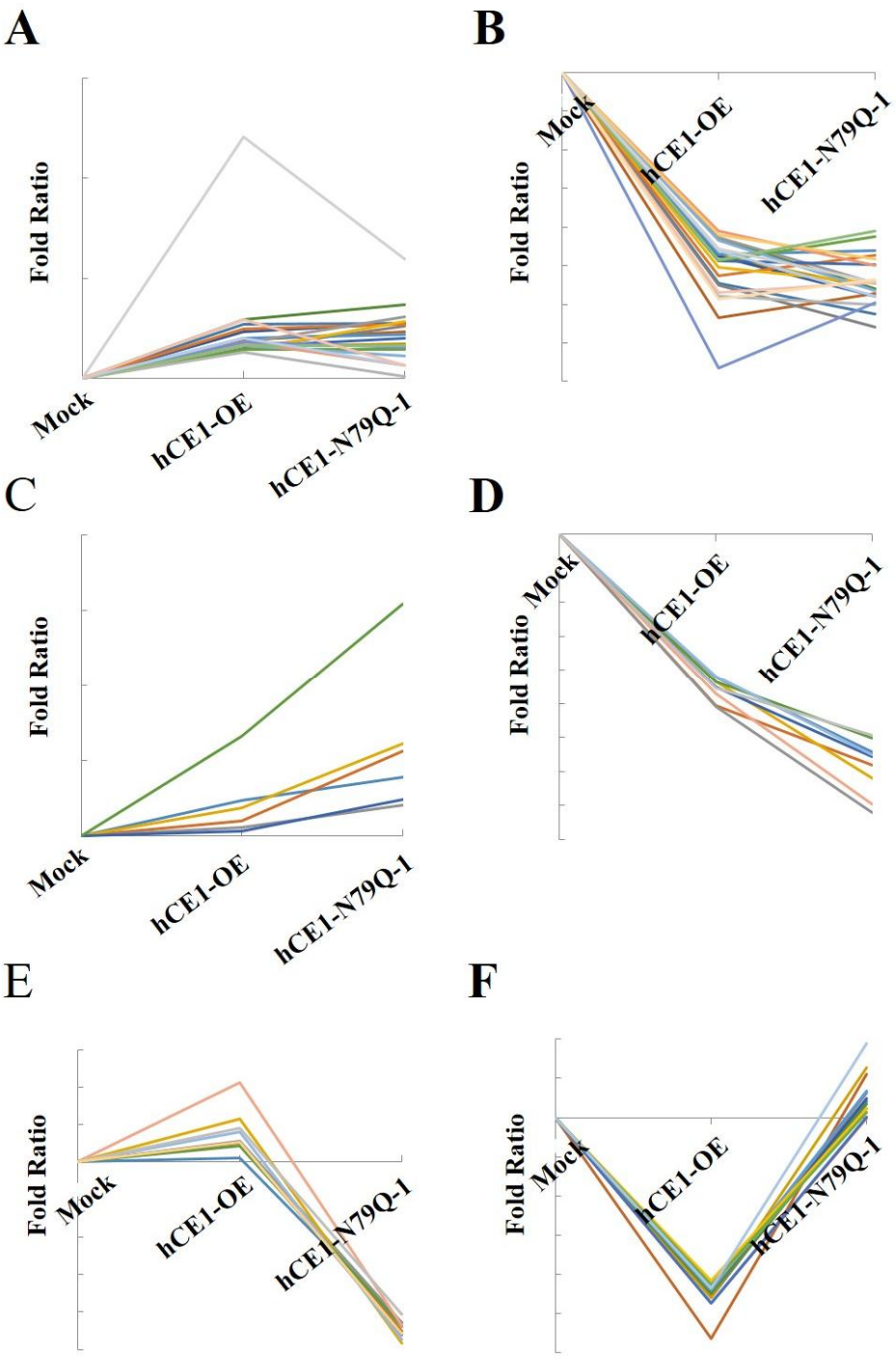

Figure 6. Six patterns for expression level of three clones.

To classify those proteins that are affected by de-glycosylation of hCE1, the 71 identified proteins were divided into six expression pattern as shown to (A)–(F).

A

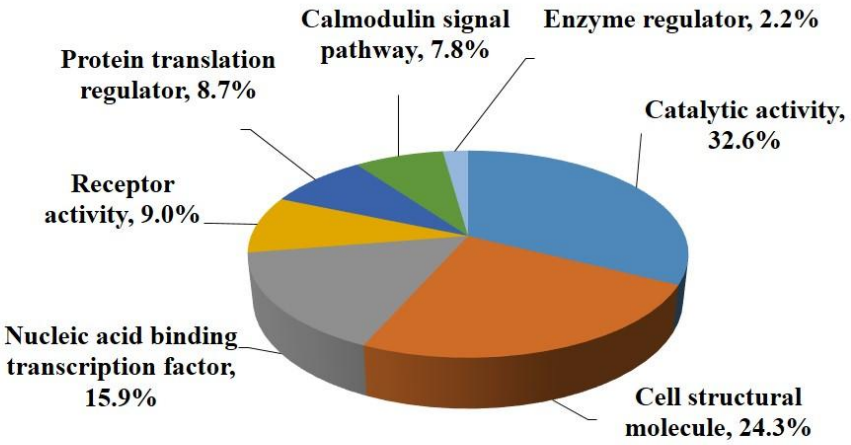

B

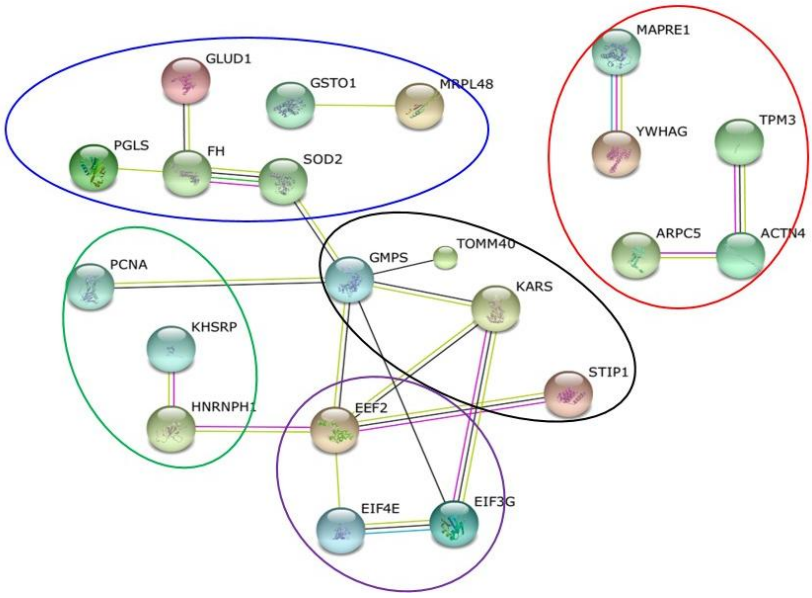

Figure 7. Protein networking and related biological functions.

(A) The major GO classifications for the molecular and biological function were analyzed by searching for the PANTHER database. (B) Seventy-one proteins were classified into colored lines by interaction type using the STRING network (v10). The original data were modified to classify the proteins. Color of lines are: blue for energy metabolism, red for cell structural molecule and proliferation, green for nucleic acid binding transcription factor, black for ATP synthesis, and purple for protein translation regulator.

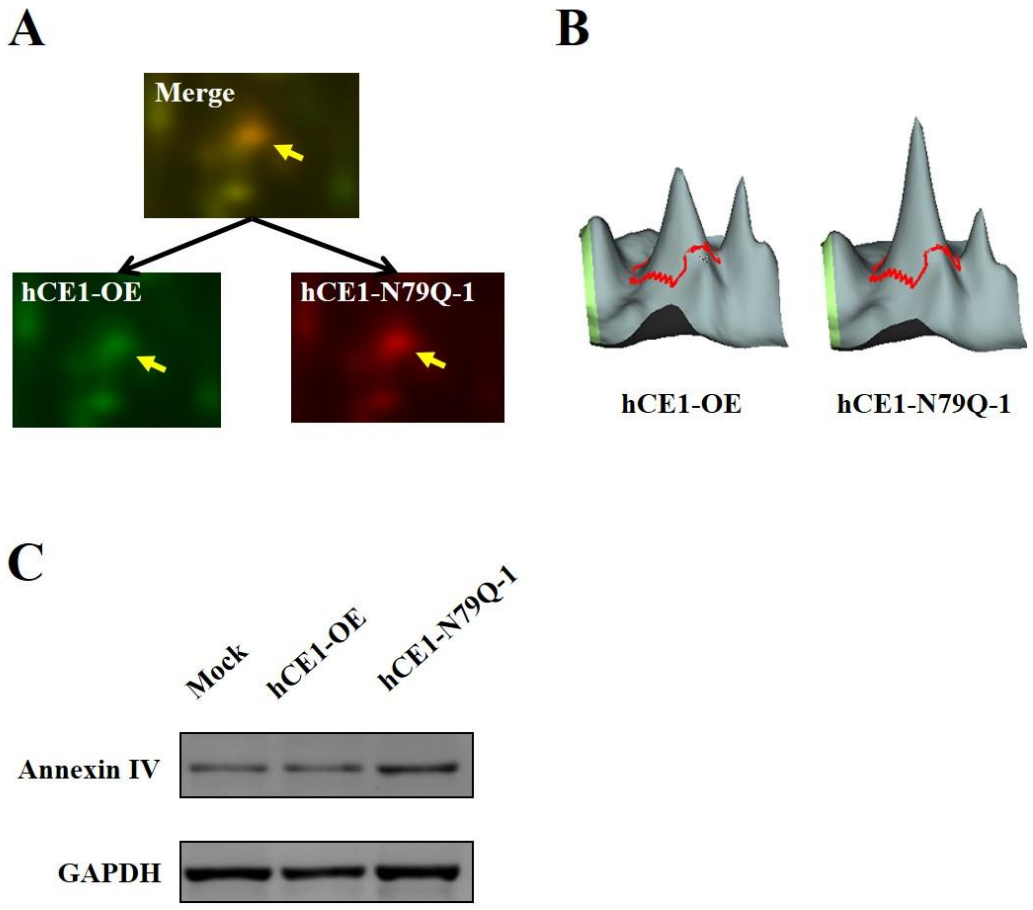

Figure 8. Confirmation of Annexin IV level in proteomics analysis.

(A) The Annexin IV spot was differentially expressed between hCE1-OE (Cy3: green) and hCE1-N79Q-1 (Cy5: red) in 2-D DIGE. (B) The intensity of each spot could be compared as 3D image. (C) To validate the 2-D DIGE result, Annexin IV level was re-analyzed by Western blot analysis (triplicate experiments).

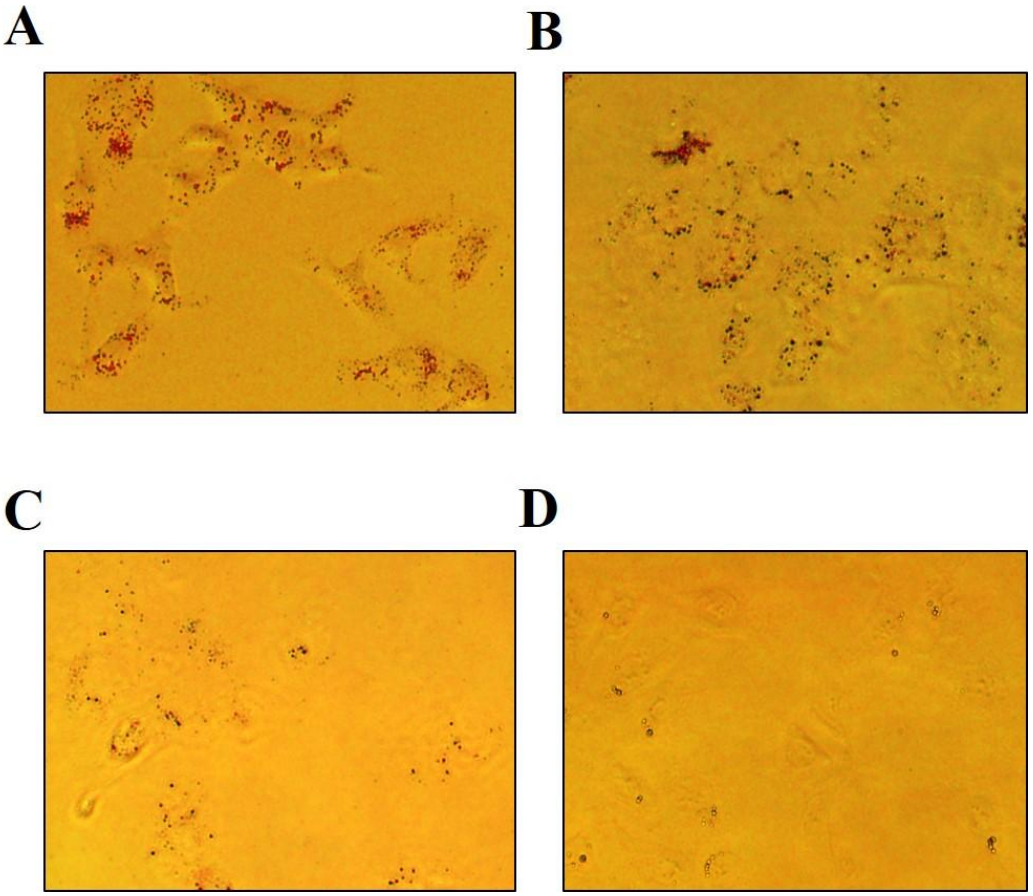

Figure 9. Comparison of cellular lipid accumulation between the mutant HCC cells.

For alternative lipid hydrolytic activity of hCE1, intracellular lipid accumulation was determined from lipid stain by Oil Red O dye. The lipid distribution of (A) Hep3B parental, (B) mock control, (C) hCE1-OE and (D) hCE1-N79Q-1 clones were captured using microscope. The red color presents lipid.

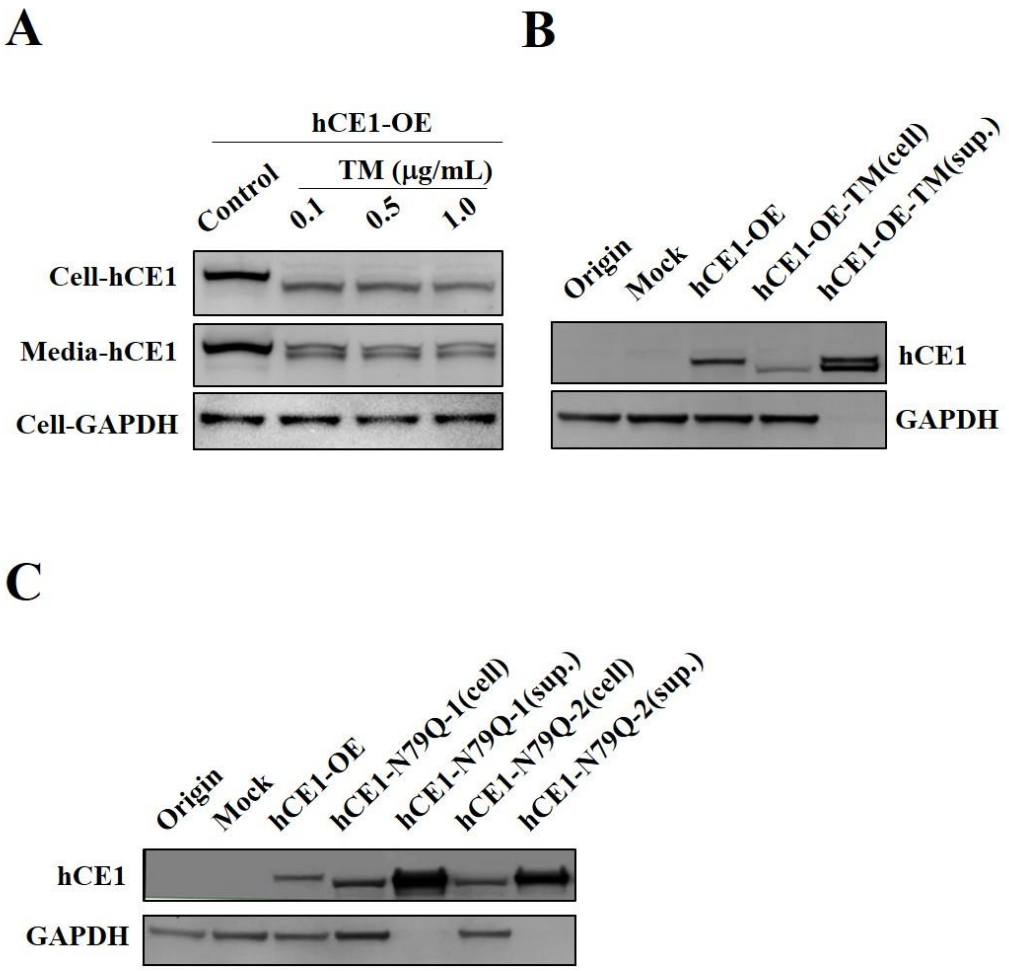

Figure 10. Effect of de-glycosylation on the hCE1 secretion by de-glycosylation.

(A) After tunicamycin (TM, 0–1.0 μg/mL) treatment of hCE1-OE cells, the cells and its supernatant (sup.) were collected or concentrated, and then each 20 μg protein was applied to Western blot analysis. TM concentration of hCE1-MW shift-down was 0.5 μg/mL. (B) Using TM-treated samples, each cell lysate of Hep3B parental, mock and hCE1-OE cells was cross-compared to validate hCE1 secretion by de-glycosylation. (C) The cell pellets or supernatant of Hep3B parental and its stable clones containing two hCE1-N79Q cells were analyzed for hCE1 secretion from cell to media on *N*-glycan mutation.

References

Altekruse S.F., McGlynn K.A. and Reichman M.E. (2009) Hepatocellular carcinoma incidence, mortality, and survival trends in the United States from 1975 to 2005. *J. Clin. Oncol*., **27**, 1485-1491

Bambang I.F., Xu S., Zhou J., Salto-Tellez M., Sethi S.K. and Zhang D. (2009) Overexpression of endoplasmic reticulum protein 29 regulates mesenchymal-epithelial transition and suppresses xenograft tumor growth of invasive breast cancer cells. *Lab. Invest*., **89**, 1229-1242

Barbara I. and Keith W.R. (1995) Conformational implications of asparagine-linked glycosylation. *Proc. Natl. Acad. Sci. USA*. **92**, 97–101

Bause E. (1983) Structural requirements of N-glycosylation of proteins. *Biochem J*., **209**, 331–336

Bence M. and Sahin-Tóth M. (2011) Asparagine-linked glycosylation of human chymotrypsin C (CTRC) is required for folding and secretion but not for enzyme activity. *FEBS J*., **278**, 4338-4350

Bennett E.P., Mandel U., Clausen H., Gerken T.A., Fritz T.A. and Tabak L.A. (2012) Control of mucin-type O-glycosylation: a classification of the polypeptide GalNAc-

transferase gene family. *Glycobiology*, **22**,736–756

Cheng L., Gao S., Song X., Dong W., Zhou H., Zhao L. and Jia L. (2016) Comprehensive N-glycan profiles of hepatocellular carcinoma reveal association of fucosylation with tumor progression and regulation of FUT8 by microRNAs. *Oncotarget*, **7**, 61199-61214

Choi H.S., Yim S.H., Xu H.D., Jung S.H., Shin S.H., Hu H.J., Jung C.K., Choi J.Y. and Chung Y.J. (2010) Tropomyosin3 overexpression and a potential link to epithelial-mesenchymal transition in human hepatocellular carcinoma. *BMC Cancer*, **10**, 122

Cox M.L. and Meek D.W. (2010) Phosphorylation of serine 392 in p53 is a common and integral event during p53 induction by diverse stimuli. *Cell Signal*., **22**, 564-71

Cuddihy A.R., Wong A.H., Tam N.W., Li S. and Koromilas A.E. (1999) The double-stranded RNA activated protein kinase PKR physically associates with the tumor suppressor p53 protein and phosphorylates human p53 on serine 392 in vitro. *Oncogene*, **18**, 2690-2702

Ebeling F.G., Stieber P., Untch M., Nagel D., Konecny G.E., Schmitt U.M., Fateh-Moghadam A. and Seidel1 D. (2002) Serum CEA and CA 15–13 as prognostic factors in primary breast cancer. *Br. J. Cancer*, **86**, 1217–1222

Elchuri S., Naeemuddin M., Sharpe O., Robinson W.H. and Huang T.T. (2007) Identification of biomarkers associated with the development of hepatocellular carcinoma in CuZn superoxide dismutase deficient mice. *Proteomics*, **7**, 2121-2129

Fleming J.M., Ginsburg E., Oliver S.D., Goldsmith P. and Vonderhaar B.K. (2012) Hornerin, an S100 family protein, is functional in breast cells and aberrantly expressed in breast cancer. *BMC Cancer*, **12**, 266

Forero-Torres A., Infante J.R., Waterhouse D., Wong L., Vickers S., Arrowsmith E., He A.R., Hart L., Trent D.,Wade J., Jin X., Wang Q., Austin T., Rosen M., Beckman R., von Roemeling R., Greenberg J. and Saleh M. (2013) Phase 2, multicenter, open-label study of tigatuzumab (CS-1008), a humanized monoclonal antibody targeting death receptor 5, in combination with gemcitabine in chemotherapy-naive patients with unresectable or metastatic pancreatic cancer. *Cancer Med.*, **2**, 925-932

Fulda S. and Debatin K.M. (2006) Extrinsic versus intrinsic apoptosis pathways in anticancer chemotherapy. *Oncogene*, **25**, 4798-4811

Gilgunn S., Conroy P.J., Saldova R., Rudd P.M. and O'Kennedy R.J. (2013) Aberrant PSA glycosylation — a sweet predictor of prostate cancer. *Nat. Rev. Urol*. **10**, 99–107

Helenius A. and Aebi M. (2001) Intracellular functions of N-linked glycans. *Science*, **291**, 2364–2369

Hsieh S.Y., Huang S.F., Yu M.C., Yeh T.S., Chen T.C., Lin Y.J., Chang C.J., Sung C.M., Lee Y.L. and Hsu C.Y. (2010) Stathmin1 overexpression associated with polyploidy, tumor-cell invasion, early recurrence, and poor prognosis in human hepatoma. *Mol. Carcinog*., **49**, 476-487

Hua S., Saunders M., Dimapasoc L.M., Jeong S.H., Kim B.J., Kim S., So M., Lee K.S., Kim J.H., Lam K.S., Lebrilla C.B. and An H.J. (2014). Differentiation of cancer cell origin and molecular subtype by plasma membrane N-glycan profiling. *J Proteome Res.*, **13**, 961–968

Hua Z., Chen J., Sun B., Zhao G., Zhang Y., Fong Y., Jia Z. and Yao L. (2011) Specific expression of osteopontin and S100A6 in hepatocellular carcinoma. *Surgery*, **149**, 783-791

Imai T. (2006) Human Carboxylesterase Isozymes: Catalytic properties and rational drug design. *Drug Metab. Pharmacokinet*., **21**, 173-185

Jemal A., Bray F., Center M.M., Ferlay J., Ward E. and Forman D. (2011) Global cancer statistics. *CA. Cancer J. Clin.*, **61**, 69-90

Ji N.Y., Park M.Y., Kang Y.H., Lee C.I., Kim D.G., Yeom Y.I., Jang Y.J., Myung P.K., Kim J.W., Lee H.G., Kim J.W., Lee K. and Song E.Y. (2009) Evaluation of annexin II as a potential serum marker for hepatocellular carcinoma using a developed sandwich ELISA method. *Int. J. Mol. Med*., **24**, 765-771

Ko B.S., Lai I.R., Chang T.C., Liu T.A., Chen S.C., Wang J., Jan Y.J. and Liou J.Y. (2011) Involvement of 14-3-3γ overexpression in extrahepatic metastasis of hepatocellular carcinoma. *Hum. Pathol.*, **42**, 129-135

Kornfeld R. and Kornfeld S. (1985) Assembly of asparagine-linked oligosaccharides. *Annu. Rev. Biochem.*, **54**, 631-664

Kroetz D.L., McBride O.W. and Gonzalez F.J. (1993) Glycosylation-dependent activity of baculovirus-expressed human liver carboxylesterases: cDNA cloning and characterization of two highly similar enzyme forms. *Biochemistry*, **32**, 11606-11617

Lederkremer G.Z. (2009) Glycoprotein folding, quality control and ER-associated degradation. *Curr. Opin. Struct. Biol.*, **19**, 515–523

Lee M.J., Na K., Jeong S.K., Lim J.S., Kim S.A., Lee M.J., Song S.Y., Kim H.K., Hancock W.S., Paik Y.K. (2014) Identification of Human Complement Factor B as a Novel Biomarker Candidate for Pancreatic Ductal Adenocarcinoma. *J. Proteome Res*. **13**, 4878-4888

Lodish H., Berk A., Zipursky S.L., Matsudaira P., Baltimore D. and Darnell J. (2000) *Molecular cell biology 4th edition*

Lu X. and Qin W. (2012) Vacuolar H(+)-ATPase in Cancer Cells: Structure, Function. *Atlas. Genet. Cytogenet. Oncol. Haematol.*, **16**, 252-259

Luo X., Xie H., Long X., Zhou M., Xu Z., Shi B., Jiang H. and Li Z. (2013) EGFRvIII mediates hepatocellular carcinoma cell invasion by promoting S100 calcium binding protein A11 expression. *PLoS One*, **8**, e83332

Mun K.S., Cheah P.L., Baharudin N.B. and Looi L.M. (2006) Proliferating cell nuclear antigen (PCNA) activity in hepatocellular carcinoma, benign peri-neoplastic and normal liver. *Malays. J. Pathol*., **28**, 73-77

Na K., Jeong S.K., Lee M.J., Cho S.Y., Kim S.A., Lee M.J., Song S.Y., Kim H., Kim K.S., Lee H.W. and Paik Y.K. (2013) Human liver carboxylesterase 1 outperforms alpha-fetoprotein as biomarker to discriminate hepatocellular carcinoma from other liver diseases in Korean patients. *Int. J. Cancer*., **133**, 408-415

Na K., Lee E.Y., Lee H.J., Kim K.Y., Lee H., Jeong S.K., Jeong A.S., Cho S.Y., Kim S.A., Song S.Y., Kim K.S., Cho S.W., Kim H. and Paik Y.K. (2009) Human plasma carboxylesterase 1, a novel serologic biomarker candidate for hepatocellular carcinoma. *Proteomics*, **9**, 3989-3999

Nakamura J., Aoyagi S., Nanchi I., Nakatsuka S., Hirata E., Shibata S., Fukuda M., Yamamoto Y., Fukuda I., Tatsumi N., Ueda T., Fujiki F., Nomura M., Nishida S., Shirakata T., Hosen N., Tsuboi A., Oka Y., Nezu R., Mori M., Doki Y., Aozasa K., Sugiyama H. and Oji Y. (2009) Overexpression of eukaryotic elongation factor eEF2 in gastrointestinal cancers and its involvement in G2/M progression in the cell cycle. *Int. J. Oncol*., **34**, 1181-1189

Ning B.F., Ding J., Yin C., Zhong W., Wu K., Zeng X., Yang W., Chen Y.X., Zhang J.P., Zhang X., Wang H.Y. and Xie W.F. (2010) Hepatocyte nuclear factor 4 alpha suppresses the development of hepatocellular carcinoma. *Cancer Res*., **70**, 7640-7651

Nonaka M., Ma B.Y., Ohtani M., Yamamoto A., Murata M., Totani K., Ito Y., Miwa K., Nogami W., Kawasaki N., Kawasaki T. (2007) Subcellular localization and physiological significance of intracellular mannan-binding protein. *J. Biol. Chem*. **282**, 17908-17920

Ohata T., Yokoo H., Kamiyama T., Aiyama T., Wakayama K., Orimo T., Kakisaka T., Tsuruga Y., Kamachi H. and Taketomi A. (2015) Effect of high expression of fatty acid binding protein 5 on prognosis and epithelial-mesenchymal transition in hepatocellular carcinoma. *J. Clin. Oncol*., **33**, 310

Ota F., Kizuka Y., Kitazume S., Adachi T. and Taniguchi N. (2016) N-glycosylation is essential for the secretion of extracellular superoxide dismutase. *FEBS Lett*., **590**, 3357-3367

Perz J.F., Armstrong G.L., Farrington L.A., Hustin Y.J. and Bell B.P. (2006) The contributions of hepatitis B virus and hepatitis C virus infections to cirrhosis and primary liver cancer worldwide. *J. Hepatol*., **45**, 529-538

Pucci S., Bonanno E., Pichiorri F., Angeloni C. and Spagnoli L.G. (2004) Modulation of different clusterin isoforms in human colon tumorigenesis. *Oncogene*, **23**, 2298-2304

Pucci S., Mazzarelli P., Nucci C., Ricci F. and Spagnoli L.G. (2009) CLU "in and out": looking for a link. *Adv. Cancer Res*., **105**, 93-113

Rajeshkumar N.V., Rasheed Z.A., García-García E., López-Ríos F., Fujiwara K., Matsui W.H. and Hidalgo M. (2010) A combination of DR5 agonistic monoclonal antibody with gemcitabine targets pancreatic cancer stem cells and results in long-term disease control in human pancreatic cancer model. *Mol. Cancer Ther*., **9**, 2582-2592

Reis C.A., Osorio H., Silva L., Gome C. and David L. (2010) Alterations in glycosylation as biomarkers for cancer detection. *J. Clin. Pathol*., **63**, 322–329

Safi F., Schlosser W., Kolb G. and Beger H.G. (1997) Diagnostic value of CA 19–19 in patients with pancreatic cancer and nonspecific gastrointestinal symptoms. *J. Gastrointest. Surg*., **1**, 106–112

Satoh T. and Hosokawa M. (2006) Structure, function and regulation of carboxylesterases. *Chem. Biol. Interact*., **162**, 195–211

Scharf J.G., Dombrowski F. and Ramadori G. (2001) The IGF axis and hepatocarcinogenesis. *Mol. Pathol*., **54**, 138-144

Schreiber R., Taschler U., Wolinski H., Seper A., Tamegger S.N., Graf M., Kohlwein S.D., Haemmerle G., Zimmermann R., Zechner R. and Lass A. (2009) Esterase 22 and beta-glucuronidase hydrolyze retinoids in mouse liver. *J. Lipid. Res*., **50**, 2514–2523

Shental-Bechor D. and Levy Y. (2009) Folding of glycoproteins: toward understanding the biophysics of the glycosylation code. *Curr. Opin. Struct. Biol*., **19**, 524–533

Siegel R., Naishadham D. and Jemal A. (2013) Cancer statistics. *CA.Cancer J. Clin*., **63**, 11-30

Skropeta D. (2009) The effect of individual N-glycans on enzyme activity. *Bioorg Med Chem*., **17**, 2645–2653

Torre L.A., Bray F.B., Siegel R.L., Ferlay J., Lortet-Tieulent J. and Jemal A. (2012) Global cancer statistics. *CA. Cancer J. Clin*., **65**, 87-108

Tomassi A.D., Pizzuti M., Traboni C. (2003) Hep3B Human Hepatoma Cells Support Replication of the Wild-Type and a 5′-End Deletion Mutant GB Virus B Replicon. *J. Virol.* **77**, 11875-11881

Trinchet J.C., Alperovitch A., Bedossa P., Degos F., Hainaut P. and Beers B.V. (2009) Epidemiology, prevention, screening and diagnosis of hepatocellular carcinoma. *Bull. Cancer*., **96**, 35-43

Tsuchiya N., Sawada Y., Endo I., Saito K., Uemura Y. and Nakatsura T. (2015) Biomarkers for the early diagnosis of hepatocellular carcinoma. *W. J. G.*, **21**, 10573-10583

Varki A., Cummings R.D., Esko J.D., Freeze H.H., Stanley P., Bertozzi C.R., Hart G. W. and Etzler M.E. (2009) *Essentials of Glycobiology 2nd edition*

Wang C., Cigliano A., Jiang L., Li X., Fan B., Pilo M.G., Liu Y., Gui B., Sini M., Smith J.W., Dombrowski F., Calvisi D.F., Evert M. and Chen X. (2015) 4EBP1/eIF4E and p70S6K/RPS6 axes play critical and distinct roles in hepatocarcinogenesis driven by AKT and N-Ras proto-oncogenes in mice. *Hepatology*, **61**, 200-213

Wang M.C., Chang Y.H., Wu C.C., Tyan Y.C., Chang H.C., Goan Y.G., Lai W.W., Cheng P.N. and Liao P.C. (2015) Alpha-actinin 4 is associated with cancer cell motility and is a potential biomarker in non-small cell lung cancer. *J. Thorac. Oncol.*, **10**, 286-301

Wang Z.G., Jia M.K., Cao H., Bian H. and Fang X.D. (2013) Knockdown of Coronin-1C disrupts Rac1 activation and impairs tumorigenic potential in hepatocellular carcinoma cells. *Oncol. Rep.*, **29**, 1066-1072

Wei B., Guo C., Liu S. and Sun M.Z. (2015) Annexin A4 and cancer. *Clin. Chim. Acta.*, **447**, 72-78

Yau W.Y., Shih H.C., Tsai M.H., Sheu J.C., Chen C.H. and Chow L.P. (2013) Autoantibody recognition of an N-terminal epitope of hnRNP L marks the risk for developing HBV-related hepatocellular carcinoma. *J. Proteomics*, **94**, 346-358

Yi W., Clark P.M., Mason D.E., Keenan M.C., Hill C., Goddard III W.A., Peters E.C., Driggers E.M. and Hsieh-Wilson L.C. (2012) Phosphofructokinase 1 Glycosylation Regulates Cell Growth and Metabolism. *Science*, **337**, 975-980

Zhang J., Niu D., Sui J., Ching C.B. and Chen W.N. (2009) Protein profile in hepatitis B virus replicating rat primary hepatocytes and HepG2 cells by iTRAQ-coupled 2-D LC-MS/MS analysis: Insights on liver angiogenesis. *Proteomics*, **9**, 2836-2845

Zhang Q., Jiang K., Li Y., Gao D., Sun L., Zhang S., Liu T., Guo K. and Liu Y. (2015) Histidine-rich glycoprotein function in hepatocellular carcinoma depends on its N-glycosylation status, and it regulates cell proliferation by inhibiting Erk1/2 phosphorylation. *Oncotarget*, **6**, 30222-30231

Zhang Y., Li Z., Yang M., Wang D., Yu L., Guo C., Guo X. and Lin N. (2013) Identification of GRB2 and GAB1 coexpression as an unfavorable prognostic factor for hepatocellular carcinoma by a combination of expression profile and network analysis. *PLos One*, **8**, e85170

Zhao Y.J., Ju Q. and Li G.C. (2013) Tumor markers for hepatocellular carcinoma. *Mol. Clin. Oncol.*, **1**, 593-598

Abstract in Korean

HCC cell line에서 human liver carboxylesterase 1의 *N*-glycosylation에 대한 기능

김 윤진

융합오믹스의생명과학과

연세대학교 대학원

Human liver carboxylesterase 1(hCE1)은 생체 약물대사에서 중요한 역할을 하며 간에서의 항상성을 위한 트리글리세라이드 가수분해와 같은 지질대사에도 연관되어 있다. *N*-, *O*-linked glycan을 포함하는 glycosylation은 단백질의 생합성 과정에서의 가장 복잡한 번역 후 변형(post-translational modification) 단계이다. *N*-glycosylation의 특정 유형은 세포의 성장, 분화 과정, 종양 생성과 전이와 같이 생물학적 기능들에 밀접하게 연관되어 있다.

hCE1의 *N*-glycan(N79)은 생체 외에서의 그 효소에 대해서도 연관이 있다고 알려져 있지만, 간암에서의 세포의 기능은 여전히 명확하게 정의되지 않은 상태다. hCE1이 간암의 새로운 바이오마커로 발견된 것을 고려하여, 간암에서 hCE1의 *N*-glycan에 대한 세포기능적 변화를 알아내고자 하였다. 이를 위하여, 기존에 구축한 hCE1이 낮게 발현되는 Hep3B origin 세포로부터 hCE1-과발현 시킨 세포를 형질주입하여 N79Q-glycan 돌연변이 세포주를

구축하였다. 이 세포주들로 프로테오믹스 비교 분석을 위해 형광 2차전기영동법(2-D DIGE)과 LC-MS/MS 실험을 진행하였다. 형광 전기영동 이미지로부터, 71개의 다르게 발현되는 단백질 스팟들을 찾았고, 확인된 단백질들은 종양억제자 또는 종양유발자로서 알려져 있었다. 흥미롭게도, hCE1-과발현 세포에서의 세포 성장 속도는 Hep3B 대조 세포보다 느린 반면, N79Q-glycan 돌연변이 세포는 hCE1-과발현 세포보다 더 빠르고, 대조 세포와 비슷하였다. 또한, hCE1의 지질 축적과 분비작용에 대한 실험으로 hCE1의 de-glycosylation이 두 표현형의 변화에 대해 관련되지 않음을 유추할 수 있었다.

결론적으로, hCE1의 *N*-glycosylation은 HCC 세포주들간에서 hCE1의 종양형성을 억제하는 데 중요한 역할을 할 수 있을 것으로 사료된다.

핵심어 : 간암, human liver carboxylesterase 1, *N*-glycosylation